Timed Digital Cascade Control of Gas-filled Tubes

Bertalan Beszédes
Obuda University
Alba Regia Technical Faculty
Székesfehérvár, Hungary
beszedes.bertalan@uni-obuda.hu
https://orcid.org/0000-0002-9350-1802

***Abstract- The* aim of this paper is to present the operation, construction, design and scientific background of a Nixie tube display, microcontroller and BCD decoder controlled RTC clock with RTC interface. The paper describes the control of old TTL devices with today's modern microcontrollers, and discusses the discharge phenomena of tubes filled with a gas mixture and the control principles of this type of display tube. The analogue circuits required for operation are also described, as well as the reception and synchronisation of the atomic clock signal.**

Keywords - Nixie tube, BCD- decimal decoder, glow discharge, RTC, real time clock, atomic clock, DCF-receiver

I. Introduction

Nowadays, there is a growing trend to revive, re-market and rethink old, obsolete, "retro" electronic devices. Priority is given to those that look good and fit into the home. Record players, electron tube amplifiers and analogue electronic noise generators and synthesizers, popular among musicians, are enjoying a renaissance.

A good example is the special wristwatch of Steve Wozniak, one of the founders of Apple, whose display was made of small Nixie tubes made for this purpose. A prominent figure in this field is Dalibor Farny, who founded his own manufactory to save the construction.

The use of programmable hybrid circuits driving Nixie tube displays in higher education effectively combines modern electronic knowledge with the historical aspects of classic display technologies. This approach enhances students' comprehensive and practical understanding by bridging the gap between contemporary circuit design and programming fundamentals with the nostalgic appeal of Nixie tubes. Moreover, such devices not only foster a deeper grasp of electronic circuits and programming but also bolster creative problem-solving skills and a commitment to technical innovation.

In the layout presented in this article, the tubes will show the time and a microcontroller controls the system. In addition to the implemented real-time clock module and atomic clock synchronization unit, this design is freely extensible, since up to alarm function and temperature sensor can be built into the system.

II. Gas-filled tubes

Already J. J. Thomson was interested in the electrical conduction and discharge of gases, for which he was awarded the Nobel Prize in Physics in 1906 [1]. If the potential difference between two conductors is sufficiently large, a flow of charge carriers is initiated between them. The flow of charge carriers can be facilitated by placing the electrodes in different media. An easily ionizable gas mixture is perfect for this purpose.

Charge carriers in the cathode collide with the atoms of the gas between the electrodes, pushing them to a higher energy state and making them conductors between the anode and cathode. This initiates the flow of electrons in the gas. Meanwhile, the gas atoms, which are trying to return to their normal energy state, emit excess energy in the visible light range. The wavelength, and hence the colour, of the photons emitted depends on the composition of the gas. If the pressure of the gas mixture is sufficiently low, ionization can occur between 100 and 200 V [2, 3]. Depending on the current intensity, different phases of gas emission can be distinguished [4, 5, 6], as illustrated in the following graph (Fig. 1.)

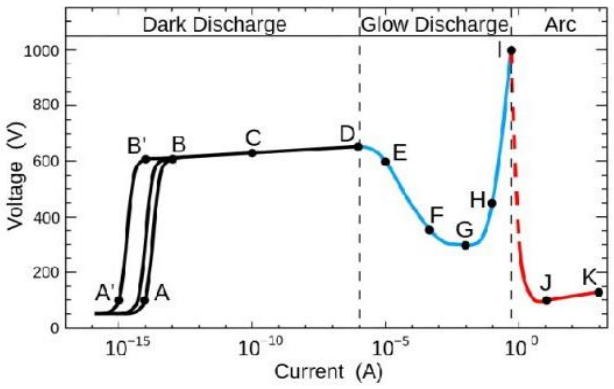

Figure 1: V-I curve of neon gas discharge in constant pressure[7]

The curve in blue shows the glow discharge section currently under discussion. At point E, the coronal discharge occurs, which can be observed, for example, in Tesla coils. At point F the glow discharge starts and stabilises at point G. In the ascending stage, an "abnormal" discharge occurs, and finally it turns into an arc discharge at point I. It can be clearly seen that the glow discharge we use occurs in the milliampere range around 300 V.

Following in the footsteps of this physical phenomenon, a pair of Hungarian brothers, George and Zoltan Haydu, developed the first Nixie tube in 1936. [8]

The tubes were kept at pressures between 0.1 and 10 Torr with a Penning mixture containing neon and argon gas. The wire-bent strings act as a cathode (-), while a wire grid in the tube acts as a common anode (+). When a sufficiently high

voltage of about 170 V is applied between the anode and a cathode, a yellowish light, a glow, is seen around the cathode.

In Figure 2, the colour of the discharge is determined primarily by the ionisation of the neon gas, but the tube also contains a blue glowing mercury vapour. This has the advantage of preventing "cathodic poisoning". If a cathode is used frequently, a layer of oxide can form on the less used electrodes next to it, which can affect its operation. This oxidation can be reduced by mercury vapour. Figure 3 shows the type of Nixie tube used in the present embodiment and its pinout.

Figure 2: Fog discharge in Nixie tube

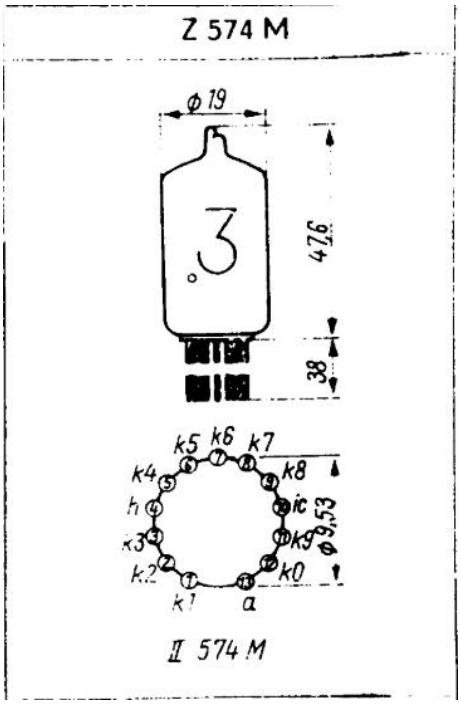

Figure 3: Construction of a Nixie tube [4]

A. Control of Nixie tubes

One of the most important part of this project is to turn on the cathodes at the right time, for the right amount of time. This can be controlled by shift registers, transistor arrays, BCD decoders. The transistor array is used to switch the high voltage, while the shift register controls the corresponding transistors depending on the input signal. If, to save space, we want to avoid the use of high voltage transistors (e.g. MPSA42), we can use HVCMOS technology shift registers, which contain all the necessary components in a DIL case (e.g. HV509) [9, 10]. General purpose BCD decoders with transistor array insertion can also be used (e.g.: HCF4028B). A low or high level given to a 4-bit (i.e. 4) input, can be mapped to a binary number, which is used by the IC to activate the output pin of the IC for the corresponding decimal value. Since the anodes are connected to the control, activation is a pull to ground potential. As an example, consider the value 5. To decode this, send 0101 ($2^0 + 2^2 = 5$) to the DCBA inputs, where "1" represents a high signal level and "0" represents a low signal level. (Note: the specific voltage values for signal levels depend on the type of IC in a given family.)

Following in this line, in 1972 Texas Instruments engineers developed a decoder specifically designed to control cold-cathode display devices (sn74141). The outputs of this IC are provided with npn transistors for switching and zener diodes to prevent negative voltage transitions (Fig. 4). This saves space, as all the necessary circuitry is contained within a DIL case. Russian equivalents of these ICs (K155ID1) are available on the market today. As the control of 6 ICs would require the control of 24 inputs according to the principle described above, multiplexing or applying GPIO expander is recommended in this case (MCP23017). There are enhanced versions of the sn74141. In addition to the 4-bit decoder, the sn74142n also includes a 4-bit memory and a counter.

It is built with MSI (Monolithic System Integration) technology. It contains four 1-bit master-slave flip-flops. To access ($\overline{\text{clear}}$) input gets low, it resets the counter and the flip-flops, then all Q outputs are low, ($\overline{Qd}$) output is high. While the $\overline{\text{clear}}$ input is inactive, i.e. high, the internal counter increments to the rising effective edge of the clock signal (clk). In ($\overline{Qd}$) output has been routed out of the package, ensuring the cascading of the ICs, thus creating the possibility of creating an n-bit counter. The Q outputs of the counter are driven to the data inputs of the latch. When the strobe input is at a low level, the latch outputs follow the counter outputs, i.e. they are always switched to a higher and higher value. If the strobe input gets high, the latch latches the previously received value. See ($\overline{Qd}$) output is not latched, as it is used to synchronize the next IC. (For cascading, the ($\overline{Qd}$) output must be driven to the clock input of the next stage.) This means that the counter of the first stage can receive new values regardless of the latch state [11].

B. Microcontroller program

An Arduino microcontroller compares the value of the RTC array loaded with the current and the previous time at given intervals, in case of a discrepancy it synchronizes the control ICs to the current time with a series of pulses (see on Fig. 5.). Similar firmware solutions can be seen in [12-16]. The microcontroller-based solutions presented here can also be applied well in technical frontier areas [17-22]. These methodologies are well connecting for higher educational

frameworks [23] and focusing on cutting-edge cybersecurity education logic [24].

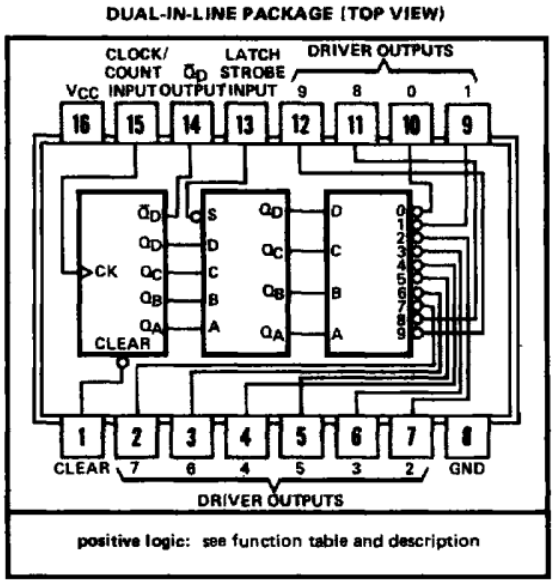

Figure 4: Internal block diagram of sn74142n [7]

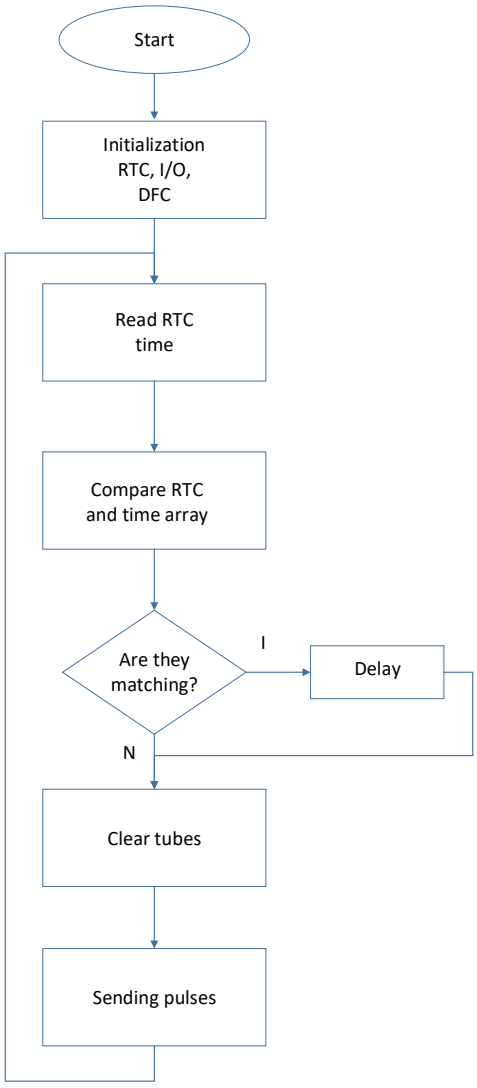

Figure 5: Main block diagram

C. Fitting a DFC module

The accuracy of the clock can be guaranteed by an atomic clock receiver, the source of which is the atomic clock in Mainflingen, Germany. The transmitter emits a long-wave signal at 77.5 KHz and adjusts the time accordingly.

DCF77 is a long-wave, 77.5 kHz AM signal that has been broadcast since 1959. The signal is transmitted on a T-antenna. The output signal power is 35 kW.

The bit sequence decoded by the receiver is generated by reducing the amplitude by 25%. If the amplitude is reduced for 100 ms, it corresponds to a logic "0". If it is reduced by 25% for 200 ms, it corresponds to logic "1". A sequence contains 60 bits. The correctness of the received signal is checked via parity bits. Parity is always even. If the parity is not correct, the received signal is not interpreted. This type of check is important because the transmitted signal is quite noisy and also attenuates with increasing distance. In terms of connection (Fig. 6), in addition to the GND and +5 V wires, the P1 enable input should be connected to GND and the T signal output to the input of the controller [25].

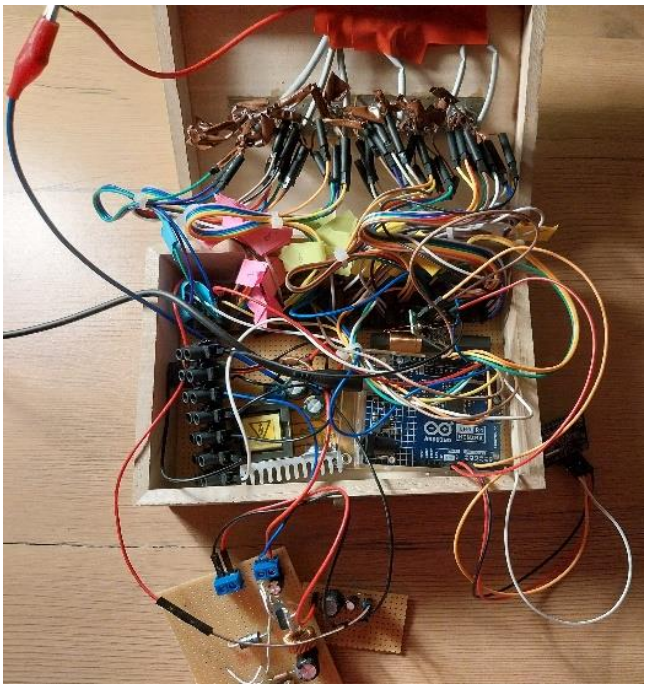

Figure 6: Connected DCF receiver with ferrite antenna hidden in the box

D. Power supply

12 V is supplied from the wall adapter, from which 170 V should be supplied to the tubes and 5 V to the ICs. I did this with a Buck and a Boost converter. The buck converter is homemade, the wiring diagram is shown in Figure 8.

The above equipment (Fig. 7.) is a possible implementation of the 170 V circuit. The anodes of the tubes are connected to the output voltage through 15 kΩ protective resistors, the cathodes are connected to the corresponding outputs of the IC. Here, the widely used MC34063 DC- DC converter has been used. The converter I used can be operated from 12 V [26].

The buck converter is capable of 12-5 V conversion, the core of which is an LM2576 DC-DC converter, shown in Figure 8.

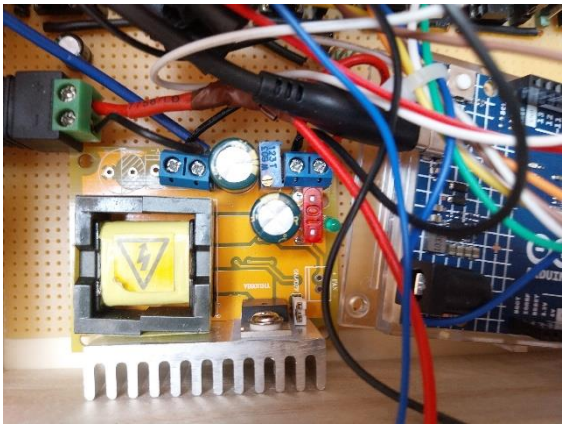

Figure 7: Boost converter module in the circuit

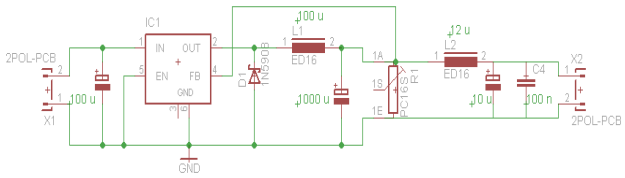

Figure 8: Buck converter circuit diagram

A common fault in switching power supplies is noise on the output voltage and voltage fluctuations. These result from the high frequency noise applied to the signal and the way the voltage is converted (the nature of switching operation). The "spikes" are short, but high amplitude voltage jumps. These characteristics are not a problem at certain loads, but in many cases they negatively affect the operation of the supplied circuit. Since I will be feeding a voltage level sensitive integrated circuit, a solution to this problem had to be found. To filter out these characteristics, an LC low-pass filter connected to the output could provide a solution. This arrangement will filter DC and low frequency signals and filters out high-frequency signals. From a scaling point of view, the breakpoint of the Bode characteristic should be scaled to a fraction of the switching frequency. The internal oscillator of the converter is 52 kHz, so at this breakpoint frequency the output signal will be attenuated appropriately. In the implementation, a coil with an inductance of 12 µH and two capacitors connected in parallel, each with 100 nF and 10 µF, were used.

III. Practical realisation

The block diagram (Fig. 9.) shows the microcontroller, with the ICs in a row below. The lower blocks are the 5 V, 170 V and 12 V sources. The RTC communicates with the controller via analog inputs A4 and A5, and the DFC receiver via digital port 13. The other digital ports are used as outputs. 6 outputs provide a clock signal, 6 provide an enable signal and 1 provides a $\overline{\text{clear}}$ signal to the ICs, which cascades through the system. These blocks receive the 5 V supply, while a 12- 170 V boost converter provides sufficient voltage to the tubes. I have used a common ground point in the system using a stub, so that the ICs ensure that the required 170 V ignition voltage is applied to the corresponding cathode of the tubes by pulling the corresponding output to ground.

When using K155ID type ICs, the connection of the microcontroller outputs is changed by adding an extra unit. The insertion of a GPIO expander array between the microcontroller and the ICs is required. This allows to expand two Arduino ports to 16 ports by communicating via I^2C protocol. Using two expander lines, instead of the "CLK, STRB lines" shown in the figure, we will need "SDA, SCL" lines to the GPIO [27]. By using two expander lines, we can provide enough connection points to transmit the corresponding binary numeric value to the 4-bit controller input of the ICs. This means that there will be four input lines to each IC. The ICs will transmit the output signals unchanged to the tubes. More serious changes are required to the microcontroller program, but there is a library for the expander that can be used to easily adapt the device [28, 29].

The components of the clock after modeling and designing [30, 31], the housing, are take a place in a 12x18 cm wooden box with custom-made sockets mounted on top (Fig. 10).

In the current design, the tubes are connected to the control system by ribbon cables, but individual spike-connectable tube socket panels are being designed, resulting in a more compact solution.

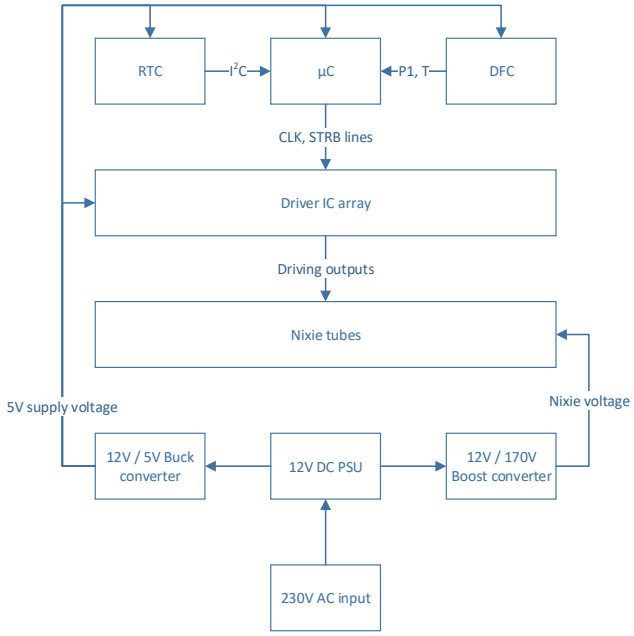

Figure 9: Block diagram of the device

Figure 10: The completed timepiece

CONCLUSION

Based on empirical experiences, integrating programmable hybrid circuits with Nixie tube displays in higher education offers a multifaceted educational tool that enriches the learning experience. This integration enables students to gain hands-on experience with both modern and vintage technologies, fostering a deeper understanding of electronic design and programming principles. Additionally, the unique appeal of Nixie tubes captivates students' interest and imagination, encouraging engagement and innovation. By bridging the gap between past and present technologies, this approach not only equips students with essential technical skills but also inspires a holistic appreciation of the evolution and future potential of electronic displays.

The development has achieved its goal, as it has been possible to convert the data sent by the RTC module into clock data, thus solving the problem of controlling the decoder ICs so that they can switch the correct cathodes on the Nixie tubes and display the correct time. Also, the developed equipment provides a good opportunity for students participating in higher education as a demonstration teaching tool to control actuators with various digital and hybrid architectures using embedded systems.

ACKNOWLEDGMENT

The authors would like to thank all the faculty staff and member that provide help and assistance throughout the project completion.

REFERENCES

[1] J.J. Thomson - Facts. NobelPrize.org. Nobel Prize Outreach AB 2024. 2024. https://www.nobelprize.org/prizes/physics/1906/thomson/facts/

[2] Weston, G.F. Cold Cathode Glow Discharge Tubes. K Barker. 1968 Phys. Bull. 20 237 DOI 10.1088/0031-9112/20/6/006

[3] Lisovskiy, V. A., et al. "Validating the Goldstein-Wehner law for the stratified positive column of dc discharge in an undergraduate laboratory." European journal of physics 33.6 (2012): 1537.

[4] Arumugam, Saravanan, Prince Alex, and Suraj Kumar Sinha. "Effective secondary electron emission coefficient in DC abnormal glow discharge plasmas." Physics of Plasmas 24.11 (2017).

[5] Betti, Maria, and L. Aldave de las Heras. "Glow discharge mass spectrometry in nuclear research." Spectroscopy Europe 15.3 (2003): 15-24.

[6] Mathew, Prijil, et al. "Experimental verification of modified Paschen's law in DC glow discharge argon plasma." AIP Advances 9.2 (2019).

[7] VacCoat. Glow Discharge Plasma Cleaning and Application. 2023.

[8] Dieter Waechter. Dieter's Nixie Tube Data Archive https://www.tube-tester.com/sites/nixie/dat_arch/RFT_book_05.pdf

[9] Motorola Inc. Semiconductor Technical Data, High Voltage Transistors, NPN Silicon, MPSA42/D Datasheet

[10] Supertex Inc. 16-Channel Serial to Parallel Converter with High Voltage Backplane Driver and Push-Pull Outputs, HV509 datasheet

[11] Texas Instruments - The TTL Data Book for Design Engineers. Second edition. 1981. LCC4112 74062-116 –AI

[12] S. Ardabili, B. Beszedes, L. Nadai, K. Szell, A. Mosavi and F. Imre, "Comparative Analysis of Single and Hybrid Neuro-Fuzzy-Based Models for an Industrial Heating Ventilation and Air Conditioning Control System," *2020 RIVF International Conference on Computing and Communication Technologies (RIVF)*, Ho Chi Minh City, Vietnam, 2020, pp. 1-6, doi: 10.1109/RIVF48685.2020.9140753.

[13] Alexander Baklanov, Svetlana Grigoryeva, György Györök. Control of LED Lighting Equipment with Robustness Elements, Acta Polytechnica Hungarica (1785-8860 1785-8860): 15 3 pp 105-119 (2016)

[14] G. Gyorok and M. Mako, "Configuration of EEG input-unit by electric circuit evolution," *2005 IEEE International Conference on Intelligent Engineering Systems, 2005. INES '05.*, Spain, 2005, pp. 255-258, doi: 10.1109/INES.2005.1555168.

[15] Aizhan Zhaparova, Dimitry Titov, Alexander Y. Baklanov, *Gyorgy* Gyorok. Study of the Effectiveness of Switching-on LED Illumination Devices and the Use of Low Voltage System in Lighting. Acta Polytechnica Hungarica (1785-8860 1785-8860): 12 5 pp 71-80 (2015)

[16] Mosavi Amirhosein, Bertalan Beszedes, Imre Felde, Nadai Laszlo, Gorji Nima E. Electrical characterization of CIGS thin-film solar cells by two- and four-wire probe technique. MODERN PHYSICS LETTERS B 2020 p. 2050102 , 16 p. (2020)

[17] S. Kimathi, B. Lantos. Modelling and Attitude Control of an Agile Fixed Wing UAV based on Nonlinear Dynamic Inversion, Periodica Polytechnica Electrical Engineering and Computer Science, Vol 66(3), 2022, pp. 227-235

[18] S. Kimathi, B. Lantos. Quaternion based attitude control of a maneuvering fixed wing UAV, IEEE 26th International Conference on Intelligent Engineering Systems (INES), pp. 261-266, 2022.

[19] I. Bendiák and T. Sándor, "Possible Ways of Measuring and Calculating Waste Heat from a Machine Diagnostic Approach," *2023 IEEE 6th International Conference and Workshop Óbuda on Electrical and Power Engineering (CANDO-EPE)*, Budapest, Hungary, 2023, pp. 000259-000266, doi: 10.1109/CANDO-EPE60507.2023.10417972.

[20] I. Bendiák and S. Semperger, "Simplified Predictive Strategy of Mechanical Life Cycle Model in Three-Phase Asynchronous Motor," *2023 IEEE 6th International Conference and Workshop Óbuda on Electrical and Power Engineering (CANDO-EPE)*, Budapest, Hungary, 2023, pp. 000267-000274, doi: 10.1109/CANDO-EPE60507.2023.10417977.

[21] I. Bendiák and T. Sándor, "Comparison of the propulsion of electric vehicles for passenger cars and buses in terms of efficiency optimization," *2021 IEEE 4th International Conference and Workshop Óbuda on Electrical and Power Engineering (CANDO-EPE)*, Budapest, Hungary, 2021, pp. 173-176, doi: 10.1109/CANDO-EPE54223.2021.9667858.

[22] Thermo-dynamic Cycle Computation of a Micro Turbojet Engine. Fozo, L; Andoga, R and Kovacs, R. 17th IEEE International Symposium on Computational Intelligence and Informatics (CINTI). 2016 17TH IEEE International Symposium on Computational Intelligence and Informatics (CINTI 2016) , pp.75-79

[23] Judit Módné Takács, Monika Pogátsnik. A Comprehensive Study on Cybersecurity Awareness: Adaptation and Validation of a Questionnaire in Hungarian Higher Technical Education. Acta Polytechnica Hungarica 21 : 10 pp. 533-552. , 20 p. (2024)

[24] Tóth Peter, Pogatsnik Monika. Advancement of inductive reasoning of engineering students. Hungarian Educational Research Journal (HERJ) 13 : 1 pp. 86-106. , 21 p. (2023)

[25] Micro Analog Systems. Time Signal Receiver Module. DAEV6180B1COB.005. 3 April, 2012

[26] Nicholas "Brent" Burns. Nixie Tube Clock Project. https://crystal.uta.edu/~burns/project_nixieclock.html (2024. 05. 07.)

[27] Microchip Technology Inc. 16-Bit I/O Expander with Serial Interface. MCP23017/MCP23S17 datasheet. DS20001952C. 2016. https://ww1.microchip.com/downloads/en/devicedoc/20001952c.pdf

[28] Bertrand Lemasle. MCP23017 Arduino reference library. https://www.arduino.cc/reference/en/libraries/mcp23017/

[29] Hajnal, Éva, Levente Kovács, and Gergely Vakulya. "Dairy Cattle Rumen Bolus Developments with Special Regard to the Applicable Artificial Intelligence (AI) Methods." Sensors 22.18 (2022): 6812.

[30] Tamás Szakács. Pneumatic Piston Control Modelling and Optimization. Acta Polytechnica Hungarica Vol. 20, No. 6, 2023. ISSN: 1785-8860

[31] Marianna Zichar. Mathability in the Fields of 3D Printing and Modeling. Acta Polytechnica Hungarica Vol. 19, No. 1, 2022. ISSN: 1785-8860